# Tensor Visualization Driven Mechanical Component Design

Andrea Kratz* — Zuse Institute Berlin
Marc Schoeneich† — Saarland University
Valentin Zobel‡ — Leipzig University
Bernhard Burgeth § — Saarland University
Gerik Scheuermann¶ — Leipzig University
Ingrid Hotz‖ — German Aerospace Center
Markus Stommel** — Saarland University


Figure 1: Design of a new rib structure for a brake lever guided by tensor lines: From design concept to virtual and experimental part tests.

**ABSTRACT**

This paper is the result of a close collaboration of mechanical engineers and visualization researchers. It showcases how interdisciplinary work can lead to new insight and progress in both fields. Our case is concerned with one step in the product development process. Its goal is the design of mechanical parts that are functional, meet required quality measures and can be manufactured with standard production methods. The collaboration started with unspecific goals and first experiments with the available data and visualization methods. During the course of the collaboration many concrete questions arose and in the end a hypothesis was developed which will be discussed and evaluated in this paper. We facilitate a case study to validate our hypothesis. For the case study we consider the design of a reinforcement structure of a brake lever, a plastic ribbing. Three new lever geometries are developed on basis of our hypothesis and are compared against each other and against a reference model. The validation comprises standard numerical and experimental tests. In our case, all new structures outperform the reference geometry. The results are very promising and suggest potential to impact the product development process also for more complex scenarios.

## 1 INTRODUCTION

Modern product development processes in mechanical engineering are governed of computer-aided simulations. That is, new technical systems are first optimized at the computer, which reduces the time-consuming and expensive real prototyping. Thereby, the growing demand for lightweight constructions requires an advanced design process. Criteria for the design of new technical systems are manifold. They include part stiffness, maximum stress peaks, weight, geometrical or functional boundary conditions and also practical aspects of manufacturability. For the validation and comparison of the performance of various design options under standard operating conditions they are simulated and analyzed. In the case of material stressing, this comparison is performed on the basis of a couple of scalar key metrics. But, the output of the simulations is much more comprehensive. It involves a variety of additional vector and tensor-valued data fields, for example, displacement vector fields and stress and strain tensor fields. Most of this data is currently considered as an intermediate product and is not used for the evaluation and improvement of the part design although it contains valuable information. One reason is the lack of appropriate analysis tools but also the complexity of the data. A more elaborate analysis is not part of the standard workflow. Especially for the visual analysis of stress tensor fields only basic visualizations are available such as contour plots of single components or color maps of derived quantities.

The presented work results from a collaboration of researchers from engineering and visualization. The goal is an elaboration of the potential of the full simulation data of material stressing. To fully exploit the power of the simulations, the data needs to be processed such that also non-scalar features are intuitively accessible for the engineer. Our focus is the analysis and visualization of the resulting stress tensor fields. The basis for the tensor field analysis is a visualization framework that uses the concept of multiple views together with brushing and linking similar to the framework presented by Kratz et al. [12]. Diagram views of expressive scalar identifiers frequently used by the engineers are linked with 3D spatial depictions of the data.

As a major result of the collaboration we recognize the significance of tensor lines and their potential value in designing *good* engineered technical parts. It is expressed in the following hypothesis that we want to discuss in this paper:

- The tensor lines for a stress tensor field (lines tangential to the principal stress) are related to the major load paths from the operating loads to the fixation points of a technical part. Hence, tensor lines can be considered as a central component in the structure design process. The guidance of the design of rib structures by selected tensor lines will result in an opti-

*e-mail:kratz@zib.de
†e-mail:m.schoeneich@mx.uni-saarland.de
‡e-mail:zobel@informatik.uni-leipzig.de
§e-mail: burgeth@math.uni-sb.de
¶e-mail:scheuermann@informatik.uni-leipzig.de
‖e-mail: ingrid.hotz@dlr.de
**e-mail:m.stommel@mx.uni-saarland.de

978-1-4799-2873-6/14 $31.00 © 2014 IEEE
DOI 10.1109/PacificVis.2014.51

mized rib structure which leads to stiffer parts using less material.

To validate this hypothesis, we use the design process of a brake lever made of plastics as a case study. We consider technical parts made of plastics as a common material when it comes to lightweight design. This case is a manageable but realistic example. The entire process starting with functional requirements up to building and testing prototypes is considered (Figure 1). In a first step, we compare the simulations of the standard and the improved design, respectively. In a second step, we verify the results experimentally by 3D printed brake levers as prototypes. The results strengthen our hypothesis:

- Brake levers with rib structures guided by tensor lines show an improved stiffness in computer simulations. Experiments with 3D printed brake levers also prove this result.

The advantage of our approach is the efficient combination of an automatic analysis with the expert's knowledge. The design process is directly supported without introducing additional steps into the traditional workflow. This is important to gain the necessary acceptance by the engineers, who often have tight deadlines. To the best of our knowledge, this is the first application of advanced tensor visualization methods in the design process of a technical part.

The paper is structured as follows. We start with the description of the application in Section 2.1. The subsequent Section 2.2 provides the necessary basics that are needed for the following sections. Section 3 discusses the related work. Section 4 summarizes the most important visualization methods applied in our case study which is described in Section 5. The paper ends with a discussion of the results in Section 6.

## 2 Application and basics

Section 2.1 describes the general setting of our case study. Section 2.2 then summarizes the basics of the physical background including stress tensors which build the basis for the proposed design optimization.

### 2.1 Background of the Case Study

Modern product development processes in mechanical engineering are characterized by an almost completely virtually tested and optimized part design with the aid of numerical simulations often based on finite element methods (FEM). Increased requirements of economical lightweight design cause the need for a precise and comprehensive analysis of the simulation results. Hereby, the structure simulation plays a prominent role. It comprises the calculation of e.g. deformations, strains, and stresses in the technical components under normal operating loads safeguarding its function. The key metrics that result from the FEM are the local strains and stresses which are derived as full three-dimensional (3D) tensors (Section 2.2). They are analyzed by an engineer with respect to the following questions:

- Can the material resist the local existing stressing condition?

- Does the material sufficiently use its capacity or is there any optimization potential?

A common routine for an engineer is the derivation of scalar quantities from the 3D tensors using an appropriate strength theory. These are then compared against a critical failure parameter that was experimentally derived on specimen of the considered material. While answering these *binary* questions, this process only exploits a small fraction of the information available from the rich output of the simulation. It is hardly suitable to efficiently guide the design process.

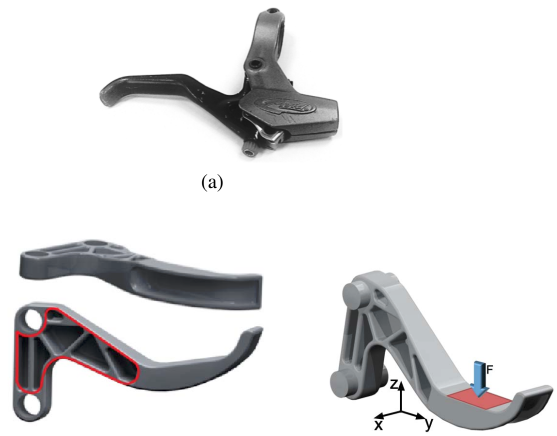


(a)

(b) (c)

Figure 2: (a) Common commercial brake lever from the manufacturer Avid. It has been used as a sample for our case study. (b) Reference geometry of a brake lever with the design space (red outlined), which is available for structural optimization. (c) FEM-simulation model with bolts for fixation and the area of the operating force application.

This paper demonstrates a new approach to utilize the full tensor data to interactively support the design process of lightweight components made of plastics material and processed by injection molding. In detail, we showcase the potential of the method exercising it for the design of a brake lever. This is an example, which is still simple enough for a suitable validation of the method. It is still fictitious and not linked to the manufacturer of the brake lever[1]. At the same time it is a realistic component, which warrants multiaxial stress conditions under the influence of the operating load. The goal is a structural optimization of the brake lever minimizing induced local stress peaks, material usage and load-dependent deformations by designing an appropriate rib structure inside a given outer geometry. The design process starts with the definition of requirements for the part. This includes the development of an initial geometry, material selection and feasibility constraints of the brake lever. It also defines the design space for the subsequent structural optimization procedure.

Material selection – The material chosen for the case study is thermoplastics. An advantage of thermoplastics in industrial applications is given by a high flexibility concerning the part shapes and by the possibility of large-scale production by the injection-molding process. In addition, the rapid prototyping with the 3D printing of plastic components enable fast results. Thermoplastics are characterized by a low density which has a positive impact on the aim of designing a low component weight.

Initial geometry – With the demand for a realistic component it is important that the component geometry can be made of plastics and that a series production process already exists. The developed outer geometry of the brake lever together with a reference rib structure to increase the component stiffness is shown in Figure 2(b). In an industrial design process the very first design of an technical part is defined either by knowledge from former parts or the designer's experience or by using common design rules that consider restrictions i.e. from the material and the production process. This geometry was designed according to common design guidelines for

[1] There has been no collaboration with the manufacturer Avid. This brake only served as a sample for a real brake lever geometry.

ribs made of plastics [7]. The red-outlined area comprises the possible design space for placing the ribs and the following structural optimization procedure.

Implementation of the Simulation – The FEM-simulation analyzing the component is performed by the commercial FEM software package Abaqus [19], which is widely used in industry for finite element analysis and computer-aided engineering. The used plastic material PBT (polybutyleneterephthalate) is described by an isotropic linear-elastic material model using a Young's modulus of 7400 MPa and a Poisson's ratio of 0.43. This simple material model is commonly used in industrial design processes of plastic parts if the loads are quasi-static and does not exceed the yield point of the material. It can be assumed that this is fulfilled for the considered brake lever under normal operating loads. The used Young's modulus is an averaged typical value of a plain PBT material and a PBT material reinforced by 20% short glass fibers. The dimensions of the component are $104 \times 15 \times 50$ mm$^3$ and the mesh resolution is 0.8 mm edge length of the finite elements. The finite elements are 10-node second-order quadratic tetrahedra, which enable a detailed geometrical representation and provide accurate simulation results. The boundary conditions to generate a realistic operating load are shown in Figure 2(c). Bolts are inserted into the brake lever to constitute the fixation of the lever during test conditions. Thus, the lever is fixed and protected from movement and torsion. The bolts are modeled with a Young's modulus of steel such that almost no deformation of fixing under load can occur. The contact between the bolt and the brake lever is modeled as frictionless to enable a rotation of the brake lever around the bolt axis.

The operating force of the braking process is applied over the highlighted plane surface (13mm $\times$ 25mm) in Figure 2(c). The simulated surface load is derived from the testing results of the hand grip test [1]. The average force exerted by a person is approximately 500 N and is used as a reference for the simulation. The simulation results contain a large variety of data including the full stress tensors.

### 2.2 Stress Tensor Fields

Given a vector space $V$, a tensor $T$ of second-order is a bilinear map $T : V \times V \to \mathbb{R}$. It is called symmetric if $T(v,w) = T(w,v)$ for any $v,w \in V$. By choosing a basis of $V$ any tensor can be represented as a matrix. In the following, we consider only tensors of dimension three with $V = \mathbb{R}^3$. Thus, they are given by $3 \times 3$ matrices. A *tensor field* on a subset $U \subset \mathbb{R}^3$ is a map that assigns each point of $U$ a 3D tensor.

Stress tensor – In this work, we are dealing with stress tensor fields. External forces applied on a body cause stresses within the body. These stresses can be described in each point of the body by a *stress tensor* $T_\sigma$, given by the respective matrix.

Since the stress tensor is symmetric, there is a basis of eigenvectors of $T_\sigma$. The eigenvectors represent the *principal stress directions*. On surfaces normal to one principal direction there act only normal stresses and no shear stresses. The magnitude of the normal stress, the *principal stress*, is then given by the corresponding eigenvalue, where positive values refer to compression and negative values to tension. According to this convention, the principal stresses in descending order are denoted by $\sigma_1 > \sigma_2 > \sigma_3$. We allude to the principal stresses and the corresponding directions as *major*, *intermediate* and *minor*, respectively. For more details, we refer to the following survey [11].

Strength Criteria – For the evaluation of the stressing of a part mostly derived scalar quantities according to some strength theory are consulted. For our case study, we use a linear-elastic isotropic model (Hooke's law). There are multiple material models suitable for different specific cases. Some models state yielding of the material when a characteristic scalar stress measure reaches a critical value: the yield strength. At this point the material starts to deform plastically (Figure 3). We consult the von Mises yield criterion

$$\sigma_v = \frac{1}{\sqrt{2}}\sqrt{(\sigma_1-\sigma_2)^2+(\sigma_2-\sigma_3)^2+(\sigma_1-\sigma_3)^2} \leq \sigma_{yield}, \quad (1)$$

which can easily be replaced by any other model when necessary.

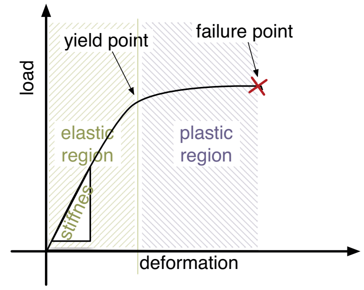


Figure 3: The slope of the load-deflection curve is an indicator for the stiffness of a technical part. It is used for the evaluation and comparison of the various brake levers designed in this case study.

Load-Deflection Curve – Another important indicator for the performance of a structure is its stiffness. Stiffness is defined as the structure's resistance to deflection. The load-deflection curve is a graphical representation of the relationship between the deflection (in the direction of the applied force) of the part and the magnitude of the applied load (Figure 3). The stiffness is indicated by the slope of the load deflection curve in its (linear) elastic region.

## 3 Related Work

Tensor Visualization in Engineering – Tensors are prevalent in many engineering applications and occur as an intermediate result in most FEM-simulations. Still, the tensor fields in their full extent are hardly considered during the analysis process. Visualizations that are commonly used in structural simulations are limited to a few simple methods. In most cases, they do not exceed the possibilities provided by the simulation or post-processing software [2, 19]. Examples are contour plots of single tensor components or of derived scalar entities. A further option is to plot the principal directions of the tensor in grid points. More advanced tensor visualization methods are unfamiliar in the mechanical engineering community. A reason might be that many visualization methods for stress tensors were not specifically designed for engineering applications. Moreover, engineers have strict time constraints so that it is not feasible for them to analyze the full simulation output.

Since tensor lines play an important role in our application, we summarize work with similar objectives or applications like ours in the following. A general overview of the state-of-the-art of tensor field visualization focusing on indefinite tensors is given in [11]. Tensor lines have been introduced as a generalization of streamlines capturing one selected eigenvector field. Extensions integrating more aspects of the tensor using its cross-section are hyperstreamlines [5]. Tensor lines have been utilized for stress tensors in a geomechanical context [16] as well as in medical applications [6]. A challenge when dealing with 3D tensor fields is to find an appropriate seeding strategy to avoid clutter and occlusion. A method called *hyperseed* that uses the anisotropy of the field has been used for DTI data [18]. In the two-dimensional (2D) case, tensor lines build the basis for sparse *stress nets* [22] or dense fabric textures [8]. We are not aware of any application of tensor lines going beyond the pure visualization purpose.

Structure optimization – The topic of structure optimization plays an important role in many engineering applications. A full review of work related to this field goes far beyond this article. We shortly summarize some major trends [17].

Manual solutions based on the experience of experts, extending or adopting existing design solutions and design rules are still widely used. These solutions are based on general design principles [13] and the experience of the engineer from previous work. But a general goal is to automate the synthesis of mechanical components as far as possible based on structural considerations fulfilling certain specifications and requirements. Design criteria include a large variety of aspects like stiffness, maximum stress peaks, weight, geometric boundary conditions and also practical aspects of manufacturability. Automated techniques dealing with this problem can be classified with respect to the chosen design variable and constraints or with respect to the chosen optimization technique.

For all these techniques there is a large body of publications varying in the optimization techniques and the description of the objective functions as well as the final geometry [15, 14]. While this is an interesting research direction, these methods have not yet found their way into the day-to-day routine workflow of an engineer designing a technical part. The optimization tools often contain many parameters which have a strong impact on the result. These parameters are not very intuitive, thus, it is hard to integrate the experts knowledge to steer the optimization process.

There has also been some work of considering major load paths for the design of structures, for example, Waldman et al. [20] and Kelly et al. [10]. The notion of load paths in this work differs strongly from ours. Instead of considering principal stress directions they define one load path for each coordinate axis, by considering the rows of the stress tensor. Thus, the definition is strongly dependent on the chosen frame of reference. This can be reasonable for geometries that can be aligned with the coordinate axis but is less useful for the more general case.

## 4 Framework for the Exploration of Stress Fields

In this section, we introduce the framework that was used in this collaboration. The framework in its entire variety (Figure 4(a)) was especially important in the beginning of the collaboration. It was needed for first data explorations that were used as a basis for regular discussions between the engineering experts and the visualization experts. These discussion lead to the hypothesis that is stated in the introduction of this paper. In the later phase, during evaluation of the hypothesis we have focused on fabric textures (Sec. 4.4), which were considered as most relevant to evaluate the hypothesis.

For the visualization and exploration of stress tensor fields, we build upon the concept presented in [12]. The idea is to use *multiple linked views* and *linking-and-brushing* for stress tensors. In the beginning of our collaboration, we combined 2D scatterplots (Sec. 4.1) and Mohr diagrams (Sec. 4.2), which are based on scalar quantities that were derived from the tensor data with 3D tensor lines (Sec. 4.3) and 2D fabric textures (Sec. 4.4). The diagram views are linked with the spatial views by a label field which is created and modified depending on selections in the scatterplot. This allows the detection of regions with specific properties in the data. In this work, brushing in the scatterplot was used to find seed points for the computation of 3D tensor lines. See Figure 4(a) for an example.

### 4.1 Scatterplots

Diagram views show the statistical distribution of properties independent of the spatial representation of the tensor field. Most important for this work were 2D scatterplots. A scatterplot has two axes, each representing one scalar value. In this work, we mapped the major $\sigma_1$ and minor $\sigma_3$ eigenvalue to the $x$- and $y$-axis, respectively. The correlation of these two variables delivers insight into central physical properties of the stress tensor field: compression, expansion and mixed stresses. See Figure 4(a) for an example. To determine seed points for the integration of 3D tensor lines, brushing of a region with high maximum shear stress $\tau_{max}$ turned out to be most relevant, these regions mostly correspond to the fixation and loading points.

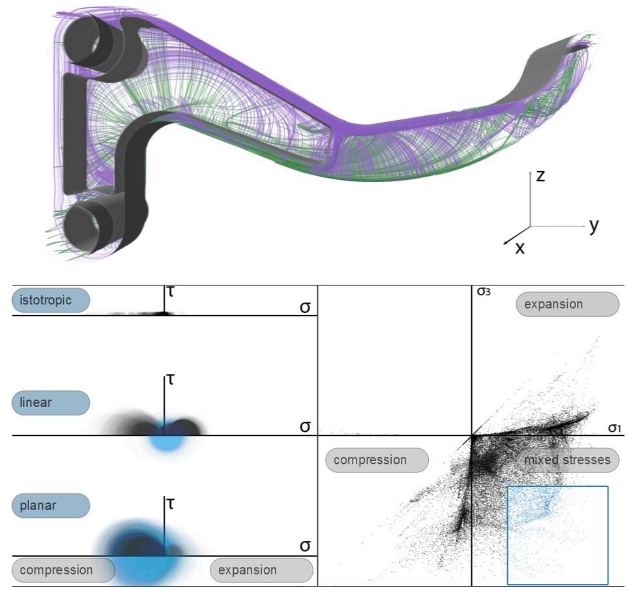


(a) Brush-and-link framework

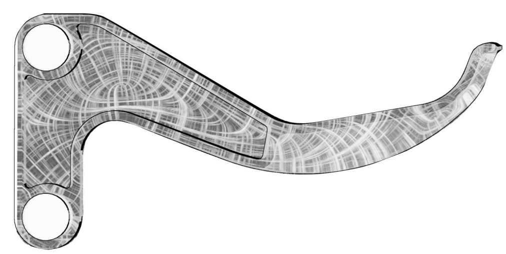

(b) Fabric texture

Figure 4: Tensor visualizations of the stress tensor field that resulted from the simulation of a brake lever. Here, the design space was filled with a solid with a Young's modulus multiple orders lower than the plastics one. (a) Brush-and-link framework (bottom right: region of highest shear selected in scatterplot, bottom left: Mohr diagram in which selected circles are displayed as full circles and others as half circles (see also [12]), top: tensor lines started at seed points that correspond to the selection in the scatterplot). (b) Fabric texture for the same dataset as in (a). The 3D lines do not significantly vary in $x$-direction. Therefore, we reduced our observations to 2D slices that are parallel to the $yz$-plane.

### 4.2 Mohr Diagrams

In the beginning of our collaboration, we also used Mohr diagrams as first presented in [4] and later adapted by [12]. As shown in Figure 4(a), we only plot the outer half-circles, which results in a histogram for stress tensors. Although Mohr circles are a familiar tool in engineering, the Mohr diagram did not lead to more insight for our application than what can already be represented by the simple scatterplot. Therefore, we later only used the scatterplot.

### 4.3 Tensor lines

One visualization method that we have used extensively in this work are tensor lines. Tensor lines play a similar role for tensor fields as streamlines for vector fields. A *tensor line* is defined as integral curve, which is tangent to one chosen eigenvector field in each point [21], [9]. For stress tensor fields they are lines following its principal directions. As there are three principal direction fields associated with the stress tensor, there are three families of tensor lines - major, intermediate, and minor principal lines. Due to the symmetry of the stress tensor, these lines are orthogonal to each other. For stress tensor fields, the major and minor principal lines are of special interest. In our context, they can be interpreted as major and minor load paths. It should be noted that tensor lines only visualize the directional information of the tensor. Similar as for streamlines one major challenge is the proper seeding of these lines. In this work, we determine seed points to compute 3D tensor lines through interactive selections in the scatterplot (Sec. 4.1).

### 4.4 Fabric Textures

To visualize 2D planar cuts through the stress tensor field, we use *fabric textures* [8] (Figure 4(b)). This is a texture-based method to visualize 2D projections of the stress field. The fabric texture represents the tensor field as a compressed, stretched and bent piece of fabric, which reflects its physical properties. The texture parameters as the fiber density and fiber direction are controlled by the principal stresses. In a first step, on basis of the stress tensor field, an anisotropic spot-noise texture is generated as input for LIC. Then, two LIC-like textures for the principal directions are created and blended, which resemble a fabric. Thinner fibers correspond to compression and thicker fibers correspond to tension. The fibers are aligned with 2D tensor lines providing a continuous representation of the principal directions. As shown in Figure 4(a) top, the 3D tensor lines do not significantly vary in $x$-direction. Therefore, we focused our observations only on 2D slices that are parallel to the $yz$-plane to evaluate our hypothesis. From this point, we did not need the whole framework anymore. Instead, we only used fabric textures as visualization method.

## 5 Optimization Steps and Results

A rib structure is the most often used reinforcement structure for injection-molded plastic parts to efficiently increase their stiffness using as less material as possible. The design of such a rib structure comprises the definition of position, number and shape of the ribs while considering given boundary conditions that follow from the manufacturing process or the part appearance. Even though there are optimization methods for some of the design steps (see Sec. 3), the design of rib structures is still mainly carried out manually by an experienced engineer. In this paper, we evaluate whether tensor visualization can assist this manual process. The idea is based on our hypothesis:

- Tensor lines can be interpreted as major load paths. That is, an optimal rib pattern should follow the tensor line pattern.

To validate this hypothesis, it needs to be proven that a rib pattern that follows a tensor line pattern offers at least the same performance in terms of the part stiffness and material stressing, than a reference lever designed without this support. A major requirement to obtain comparable results is that the amount of material is the same for all parts and that they can be manufactured with standard methods. In this work, we used injection molding of the same complexity like the reference part. As a reference part, we use a rib structure that was designed manually in accordance with the standard design rules [7] by an expert.

In the following, we describe how tensor visualization (Section 4) supported the design of new rib structures for a brake lever. We start with the description of the design process in Section 5.1. The resulting rib structure is then evaluated using a numerical FEM-simulation (Section 5.2) as well as by real prototyping (Section 5.3) in an experimental study.

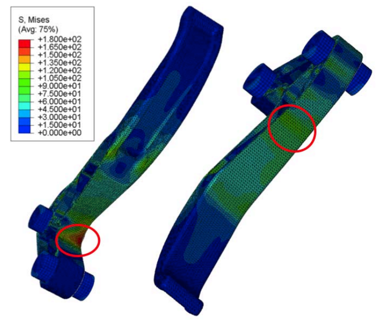


Figure 5: FEM-simulation results with highlighted maximum stress.

(a) Geometry 1

(b) Geometry 2

(c) Geometry 3

Figure 6: Simple hand sketched lines following tensor lines used as basis for three new CAD-structures.

### 5.1 Tensor-Line-Guided Design of New Rib Structures

For the design of new rib structures, we start with a reference part that was designed manually by an expert. It is shown in Figure 2(b). The outer geometry of the brake lever is predefined by mechanical and ergonomic constraints. The interior part - the design space - offers flexibility for the specific rib design. The design space is outlined in red in Figure 2(b). For the first simulation we fill this vol-

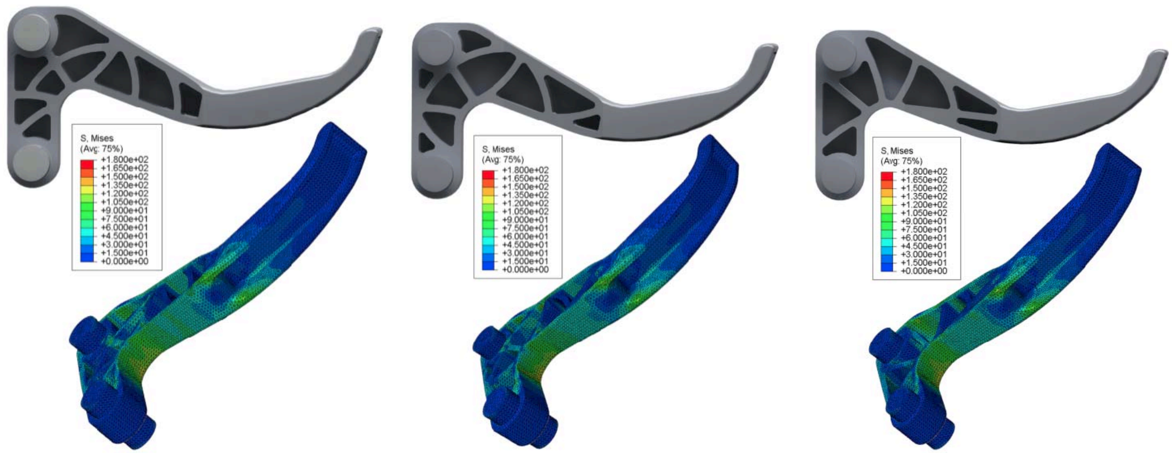


(a) Geometry 1 (b) Geometry 2 (c) Geometry 3

Figure 7: CAD models of the three rib structures designed along tensor lines and the corresponding FEM-simulation results. The maximum von Mises stresses are 126.5 MPa (1), 139.5 MPa (2), 134.4 MPa (3).

ume with a fictitious material. This allows calculating the natural run of the tensor lines that represent the flow of load from the area of operating force application to the fixation of the brake lever without imposing geometric restrictions. To not disturb the mechanics of the remaining brake lever, the Young's modulus of this fictitious material is set to a value several orders of magnitude lower than the PBT material. The material values, as well as the boundary conditions of the FEM-simulation outside the design space, remain unchanged. The operation load corresponds to the settings described in Section 2.1.

Figure 5 gives a first impression of the results of the FEM-simulation run for the brake lever. It shows the von Mises stresses visualized with the post-processing software of Abaqus. It gives a rough impression where the stresses reach their most critical value.

In a second step, ribs are designed in accordance to the tensor line pattern that is revealed by the fabric textures. Thicker lines are preferred, because they represent higher principal stresses. This is shown in Figure 6, where three different rib patterns are sketched. By designing three completely different rib patterns, we want to assess the sensitivity of the proposed method with respect to the selection of tensor lines. Similar to the usual workflow, the engineer can design the rib structure using at first hand sketches that are then transferred into the CAD-model for the simulation (Figure 7, top row). The explicit choice of the tensor lines is left to the engineer and is in accordance to his expert knowledge, which influences the number, thickness and position of the ribs. For the final CAD-models that were derived from these sketches, the total volume is 2.206% (1), 0.849% (2) and 2.096% (3) less than the volume of the reference geometry.

### 5.2 Virtual Validation of the Developed Rib Structure

First, we investigated the rib pattern by virtual test runs using the finite element method. The calculated von Mises stress of the new geometry is color-coded in Figure 7. With this visualization, the results for the three geometries are hardly distinguishable. Figure 8 shows the calculated von Mises stress in comparison to the reference part. All tensor-line-driven rib patterns show comparable von Mises stresses that are significantly lower (up to 27%) than the reference rib structure. The finite element analysis also shows an increased stiffness of the tensor-line-driven rib pattern, with a lower deformation (on average 8%) for the new brake-lever geometry under the same load.

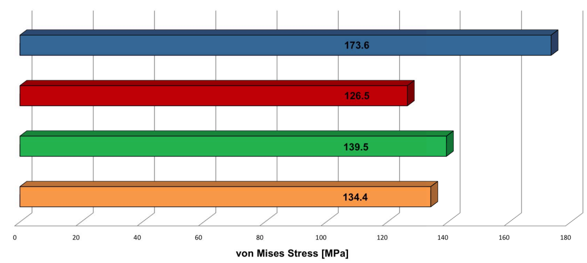


Figure 8: Resulting maximum von Mises stresses based on the FEM-simulation for the three new designs (red, green, yellow) in comparison with the reference geometry (blue).

### 5.3 Rapid Prototyping and Experimental Validation

The results presented in Section 5.2 were also investigated by real tests on prototypes generated by a rapid prototyping process. Parts generated by rapid prototyping are not usable for absolute values of properties like failure but they can be used to compare the part stiffness of different part design in a comparative way. Figure 9 shows the rapid prototype models of the reference part and the three parts with the tensor-line-driven rib structure. Figure 10 shows the test setup in a standard tensile test machine. Figure 11 shows the measured force-deflection-curves for the parts. It can clearly be stated that the three tensor-line-driven alternative designs show a comparable stiffness that is higher than the one of the reference part.

## 6 Discussion and Future Work

This paper discusses the results of a collaboration of mechanical engineers with visualization scientists.

For the engineers, a major outcome has been a hypothesis that can substantially support the design process of technical parts. The results of the finite element simulations and the experiments presented in Section 5 give evidence that tensor lines are valuable for the design of rib patterns. By selecting three different rib patterns, all based on tensor visualizations using fabric textures, we could show that our proposed method is quite robust with respect to the selected tensor lines. This makes the precise selection of the *right*

Figure 9: 3D printed new brake lever geometries

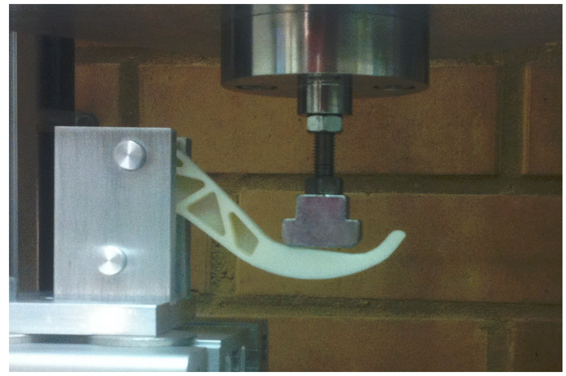

Figure 10: Test setup with fixed brake lever

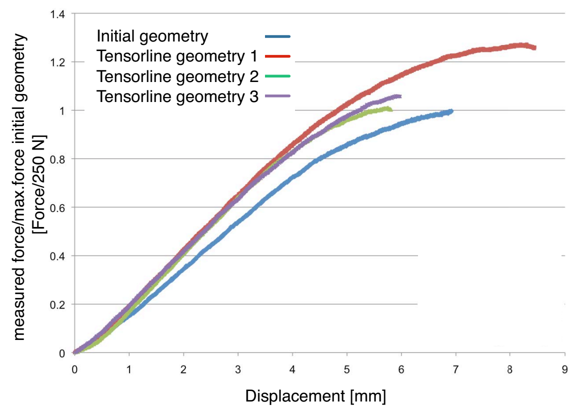


Figure 11: Load-deflection curve s of the initial geometry in comparison with the tree tensor line driven parts.

tensor lines less critical and justifies our explorative approach for the selection of tensor lines. However, for the future more in-depth evaluation is planned to verify our hypothesis. An advantage of the method proposed in this paper is that it has the potential to be easily integrated into the usual workflow of an engineer. It serves as an assistance for the usual hand-sketching design. That is, no additional simulations and tools are required to generate the additional tensor information. The stress tensor fields are already generated with the standard simulation during the design process of a technical part. They have just not been considered in the past. In a next step, we plan to further investigate our workflow by comparing its performance to the mostly iterative methods to find optimal rib patterns. Follow-up experiments with brake levers produced by injection molding as well as a comparison to computational optimization tools are planned for the future.

The application of visualization methods in the context of a specific engineering application also advances visualization research for stress tensor fields. In contrast to the area of diffusion tensor imaging (DTI), tensor lines for stress tensor fields have gained very little attention in the past. Examples are the work of [8, 22, 6]. Tensor lines have often even been considered as 'nice to have' but not useful. With the design of rib structures, we present an application for which tensor lines seem to have a high relevance and, hence, moves them back into the center of attention. By now, our approach still relies on the experience of an expert. The tensor lines that guide the design of the rib structures are selected by an engineer. His knowledge is extended by the stress tensor visualizations using fabric textures. For the future, it is important to evolve specific *importance measures* that automatically identify specific lines and further support the engineer in selecting lines for the design of the rib structure. The development of such measures will lead to exciting new challenges for tensor visualization that will result in automatic feature extraction methods.

We started our collaboration without having a specific application in mind. In this very beginning, an undirected visualization approach was necessary [3]. With the help of an explorative visualization framework (Section 4) and frequent discussions between the experts, we were able to formulate a hypothesis and to identify an application, which both were presented and evaluated in this paper. Since the results are very promising, a long-term goal is to create a visualization tool that is specifically designed for the purpose of designing rib structures and that can be used by the engineers in their daily work.

## Acknowledgements

This work was partially funded by the Saarland research funding program, Germany (Landesforschungs-Förderprogramm LFFP). Gerik Scheuermann and Valentin Zobel acknowledge the support by the ESF Nachwuchsgruppe "Visuelle Analyse für Natur- und Technikwissenschaften" (Project No. 100098251).

## REFERENCES


[1] Camry electronic hand dynamometer instruction manual.

[2] Tecplot, inc.: software for the scientific visualizations. http://www.tecplot.com/.

[3] D. Bergeron. Visualization reference model (panel session position statement). In *Proceedings of the Conference on Visualization (Vis'93)*, pages 337–342, 1993.

[4] P. Crossno, D. H. Rogers, R. M. Brannon, D. Coblentz, and J. T. Fredrich. Visualization of Geologic Stress Perturbations Using Mohr Diagrams. *IEEE Transactions on Visualization and Computer Graphics*, 11(5):508–518, 2005.

[5] T. Delmarcelle and L. Hesselink. Visualizing Second-Order Tensor Fields with Hyperstreamlines. *IEEE Computer Graphics and Applications*, 13(4):25–33, 1993.

[6] C. Dick, J. Georgii, R. Burgkart, and R. Westermann. Stress Tensor Field Visualization for Implant Planning in Orthopedics. *IEEE Transactions on Visualization and Computer Graphics*, 15(6):1399–1406, 2009.

[7] G. Erhard. *Designing with Plastics*. Carl Hanser Verlag, 2006.

[8] I. Hotz, L. Feng, H. Hagen, B. Hamann, B. Jeremic, and K. I. Joy. Physically Based Methods for Tensor Field Visualization. In *VIS '04: Proceedings of IEEE Visualization 2004*, pages 123–130. IEEE Computer Society Press, 2004.

[9] B. Jeremic, G. Scheuermann, J. Frey, Z. Yang, B. Hamann, K. I. Joy, and H. Hagen. Tensor Visualization in Computational Geomechanics. *International Journal for Numerical and Analytical Methods in Geomechanics*, 26:925–944, 2002.

[10] D. Kelly, C. Reidsema, Bassandeh, G. Pearce, and M. Lee. On Interpreting Load Paths and Identifying a Load Bearing Topology From Finite Element Analysis. *Finite Elements in Analysis and Design*, 47(8):867–876, 2011.

[11] A. Kratz, C. Auer, M. Stommel, and I. Hotz. Visualization and Analysis of Second-Order Tensors: Moving Beyond the Symmetric Positive-Definite Case. *Computer Graphics Forum - State of the Art Reports*, 32(1):49–74, 2013.

[12] A. Kratz, B. Meyer, and I. Hotz. A Visual Approach to Analysis of Stress Tensor Fields. In *Scientific Visualization: Interactions, Features, Metaphors*, volume 2 of *Dagstuhl Follow-Ups*, pages 188–211. Schloss Dagstuhl–Leibniz-Zentrum fuer Informatik, 2011.

[13] P. Y. Papalambros and D. J. Wilde. *Principles of Optimal Design: Modeling and Computation*. Cambridge University Press, 2nd edition, 2000.

[14] J. Paris, I. Colominas, F. Navarrina, and M. Casteleiro. Parallel Computing in Topology Optimization of Structures With Stress Constraints. *Computers and Structures*, 125:62–73, 2013.

[15] W. Saleem and F. Yuqing. Strategy for Optimal Configuration Design of Existing Structures by Topology and Shape Optimization Tools. *International Journal of Aerospace and Mechanical Engineering*, 4(4):226–234, 2010.

[16] G. Scheuermann, J. Frey, H. Hagen, B. Hamann, B. Jeremic, and K. I. Joy. Visualization of Seismic Soils Structure Interaction Simulations. In *VIIP*, pages 78–83, 2001.

[17] A. Schumacher. Topology Optimization of Crash-loaded Structures - Research State of the Art. In *Proceeding of the Automotive CAE Grand Challenge'13*, 2013.

[18] H.-W. Shen and A. Pang. Anisotropy Based Seeding for Hyperstreamline. In *Proceedings of IASTED International Conference on Computer Graphics and Imaging (CGIM'04)*, 2004.

[19] D. SYSTEMS. Simulia realistic simulation – abaqus: software suite for finite element analysis and computer-aided engineering,.

[20] W. Waldman, M. Heller, R. Kaye, and L. R. F. Rosen. Advances in Structural Loadflow Visuisation and Applications to Optimal Shapes. Technical Report DSTO-RR-0166, Airframes and Engines Division Aeronautical and Maritime Research Laboratory, Melbourne, Australia, 1999.

[21] D. Weinstein, G. Kindlmann, and E. Lundberg. Tensorlines: Advection-diffusion Based Propagation Through Diffusion Tensor Fields. In *VIS '99: Proceedings of the IEEE Visualization conference 1999*, pages 249–253. IEEE Computer Society Press, 1999.

[22] B. E. Wilson. *Rich Visualizations from Discrete Primitives*. PhD thesis, University of California Davis, 2005.